Graefe's Archive for Clinical and Experimental Ophthalmology (2018) 256:1653–1660
https://doi.org/10.1007/s00417-018-4069-7

BASIC SCIENCE

The influence of hydration on different mechanical moduli of the cornea

Theo G. Seiler[1,2,3] · Peng Shao[1] · Beatrice E. Frueh[2] · Seok-Hyun Yun[1] · Theo Seiler[3]

Received: 6 March 2018 / Revised: 13 June 2018 / Accepted: 12 July 2018 / Published online: 24 July 2018

Abstract

Purpose To determine the interrelation of different elastic moduli of the cornea and to investigate their dependency on corneal hydration.

Methods Rabbit eyes were divided into four groups. Corneas were excised and mounted into a Barron artificial anterior chamber. Various corneal hydration steady states were achieved with different dextran T-500 concentrations in the anterior chamber, as well as on the corneal anterior surface. The treatment-solutions of each group contained either 5, 10, 15, or 20% *w*/*w* dextran. Ultrasound pachymetry was used to measure central corneal thickness. Brillouin microscopy of the central cornea determined the longitudinal bulk modulus by means of Brillouin frequency shift. Subsequently, a 5-mm-wide central strip was taken for extensiometry to measure the tangential elastic modulus.

Results The longitudinal bulk modulus was 1.2-times higher in corneas dehydrated with 20% dextran compared to those hydrated with 5% dextran. In contrast, the tangential elastic modulus increased by 4.4 times. The obtained longitudinal bulk moduli were two orders of magnitude bigger than the tangential elastic moduli. Regression analysis of longitudinal bulk modulus and tangential elastic modulus revealed a quadratic relation. The bulk modulus seemed to be independent of tension, whereas the elastic modulus was tension-dependent. Greater corneal hydration led to significantly thicker pachymetry.

Conclusion Corneal biomechanics are highly dependent on the level of corneal hydration. Surprisingly, tangential elastic moduli were more sensitive to hydration changes than longitudinal bulk moduli. A quadratic relation was found between both moduli.

Keywords Cornea · Biomechanics · Hydration · Brillouin · Stress strain · Extensiometry · Tangential elastic modulus · Longitudinal elastic modulus

Introduction

During swelling, biological tissue incorporates water and increases its volume in all three dimensions. In contrast, swelling of the cornea happens predominantly in one dimension: it is the thickness that becomes bigger [1]. This indicates that the microscopic ultrastructure and consequently, the biomechanical constants in direction of the symmetry axis may be different from those in the corneal plane [2]. Therefore, the human cornea appears not to be an isotropic tissue but a so-called vertical transverse isotropic material [3]. Such materials are frequently modeled in geoscience [4] but have only rarely been adapted to corneal biomechanics [3].

The elastic properties of a material are described mathematically by the 4-dimensional stiffness tensor including 81 parameters. Fortunately, these 81 parameters can be reduced to 2 in isotropic material (elastic modulus and shear modulus) and to 5 in vertical transverse isotropic materials [4]. When reviewing the published results regarding elastic parameters of the cornea, we and others found a huge variation with a range of four orders of magnitude and more [5, 6]. This is not surprising because many different techniques were used measuring different parameters: one- or two-dimensional extensiometry measuring stress-strain behavior parallel to the corneal surface defining the surface-parallel (tangential) components of the elastic modulus E [7–15], indentation or

In parts presented at the 115th annual meeting of the DOG in Berlin in 2017.

✉ Theo G. Seiler
theo@seiler.tv

[1] Wellman Center for Photomedicine - Massachusetts General Hospital, Harvard Medical School, Harvard University, 50 Blossom Street, Boston, MA 02114, USA

[2] Universitätsklinik für Augenheilkunde, Inselspital, 3010 Bern, Switzerland

[3] Institut für Refraktive und Ophthalmo-Chirurgie (IROC), Stockerstrasse 37, 8002 Zürich, Switzerland, http://www.iroc.ch

compression measurements to determine the surface-perpendicular (radial, longitudinal) component of the elastic modulus [16–20], inflation experiments detecting another surface-parallel elastic modulus [13–15, 21–24]. Brillouin microscopy measuring the bulk elastic modulus M perpendicular to the surface [17, 18, 25, 26], shear spectroscopy measuring the dispersion of the shear modulus G parallel to the surface [27, 28], and mixtures of extensiometry inflation experiments and indentation measuring in an undefined direction [29]. It has been suggested that E, M, and G of the cornea are related [25, 30], but a scientific proof is still pending.

Another factor that contributes to the substantial variability of results is the hydration of the cornea [11, 23]. In many papers investigating corneal biomechanics, corneal hydration is only barely controlled [10, 11, 13] or not controlled at all [8, 9] although some studies indicate that biomechanical properties may be negatively correlated to corneal hydration [11, 23].

A noninvasive preoperative measurement of elastic properties of the cornea would help to predict the results of corneal procedures and the precision of intraocular pressure (IOP) measurements [6]. So far, such a measurement is clinically not available; however, Brillouin microscopy is a promising technique to measure elastic parameters noninvasively [25, 26, 31]. It is not decided whether such a determined bulk elastic modulus M can be used to predict the outcome of corneal operations, nor is it easily implemented in numerical or analytical corneal models.

The motivation for this study is to investigate systematically the influence of corneal hydration on surface-parallel biomechanical moduli E (by means of mechanical extensiometry) and on the bulk modulus M perpendicular to the surface (by means of Brillouin microscopy) and to see whether E and M are changing correspondingly.

Materials and methods

Sample preparation

Twenty-seven adult (12 to 24 months of age) New Zealand White frozen rabbit eyes (Pel-Freez Biologicals, Roger, AR, USA) were thawed in air. The epithelium was removed using a blunt hockey knife. According to the location of the muscle insertions and the optical nerve, the vertical axis of the cornea could be identified and marked using a waterproof pen. Corneoscleral disks were excised and mounted on an artificial anterior chamber (Barron Precision Instruments, Grand Blanc, MI, USA). Inside the chamber as well as in a reservoir on top of the cornea, a dextran-containing solution of variable dextran concentration was applied so that the osmotic agent could interact with both sides of the cornea. The artificial anterior chamber was pressurized to an equivalent IOP of 20 mmHg. Corneal pachymetry was measured by an ultrasound pachymeter (SP-100; Tomey, Nagoya, Japan) until a steady state was established (less than 5% change in three consecutive measurements 5 min apart) which took approximately 90 min. The "aqueous" dextran T-500 concentrations applied were 5, 10, 15, or 20% (Dextran from Leuconostoc spp., M_r 450,000 to 650,000, Sigma-Aldrich Corp., St. Louis, MO, USA), defining the four study groups, six eyes each. A fifth group consisted of three corneas using a dextran concentration of 13% (pachymetry close to the physiological value) to test a possible IOP dependency of the longitudinal Bulk modulus. All experiments were performed at a temperature of 19 °C. The corresponding hydration H [g water/g dry tissue] of the cornea was determined using the linear relationship

$$H = 8.65\,t - 0.62 \quad (1)$$

between corneal thickness t (mm] and hydration found by Hedbys and Mishima for rabbit cornea [32].

Brillouin microscopy

Data were acquired with a custom-made Brillouin scattering microscopy system. The system takes advantage of the spontaneous Brillouin scattering effect. When photons hit the corneal tissue, a fraction of the incident light is scattered from acoustic wavelets (naturally present in matter at room temperature) and experiences a subtle spectral shift, the so-called Brillouin frequency shift. This shift is related to localized elasticity. The system consists of a near-infrared continuous wave diode laser 780 nm (DL Pro, Toptica Photonics AG, Gräfelfing, Germany) a highly dispersive two-stage virtually imaged phased array (VIPA)-based spectrometer and a human scanning interface sitting on a slit-lamp platform. The anterior chamber was mounted with the corneal symmetry axis parallel to the incoming near-infrared light. In order to adjust intraocular pressure, the aqueous was connected to a reservoir with a variable height (range = 0 to 2 m). The light beam is focused by an objective lens (NA = 0.42, Mitutoyo, Kawasaki, Japan) to a confined focus in the stroma, and the backscattered light is collected with the same lens in a confocal fashion. Collected photons are then delivered with an optical fiber to the spectrometer, recorded by an electron multiplying charge-coupled device (EMCCD, Andor Technology, Belfast, UK) for analysis. The scanning interface can be moved manually with a joystick to define scanning locations on the cornea surface and axial scanning from anterior surface to aqueous humor in the anterior chamber is accomplished automatically by a motorized stage carrying the objective lens and thus the light focus. Lateral and axial resolutions of the system are ~ 5 and ~ 35 μm, respectively. Axial scanning was carried out with a step size of ~ 30 μm. Five central axial scanning profiles were taken of each cornea. Mean values of the Brillouin frequency shift of the stroma were calculated for each scan, and the

average of all five scans was reported for each cornea. Light power measured entering the cornea was 5 mW and a 0.7-s integration time was used for data collection with the EMCCD.

Surface-parallel Extensiometry

The corneoscleral disks were removed from the artificial anterior chamber and a cornea strip was excised using two parallel razor blades with a width of 4.9 mm in the pre-marked horizontal orientation with a total length of the strips of 10 ± 1 mm. The scleral rim was removed after the excision of the strip. The sample was then clamped horizontally at a distance of 3.0 mm between the two jaws of the extensiometer (eXpert 4000, Admet, Norwood, MA, USA). To expose the tissue to the physiological stress range as well as to establish the same equilibrium starting conditions, a force of 30 mN was applied for 100 s. In a second cycle, the force was reduced to 10 mN, at which the distance between the jaws was determined as the initial length. Subsequently, the strain was again increased linearly with a velocity of 0.017 mm/s similar to previous experiments [7, 11, 14] and the force was measured every 10 ms until a force of 6 N was detected. Stress was calculated by dividing the force at a certain strain by the cross-section area of the sample (thickness obtained from ultrasound pachymetry multiplied by width of 4.9 mm). The experiment was conducted in a moist chamber to prevent hydration changes due to evaporation. The data sets were exported and evaluated using MS Excel.

Numerical analysis

Because the stress-strain relation of the cornea is nonlinear, the tangential elastic modulus E^* varies with the level of stress and may be determined as the first derivative $d\sigma/d\varepsilon$ of the stress-strain curve at a certain strain ε_0. Since the Brillouin frequency shift was independent of surface-parallel strain up to 6%, we selected $\varepsilon_0 = 0.06$. The thus determined tangential elastic modulus E^* was compared with the longitudinal Bulk modulus M (Appendix A).

Comparison of the stress at certain strains between the four groups were performed using the Mann-Whitney U test. Best-fit functions, polynomial as well as exponential, were obtained using regression analysis and the coefficient of determination R^2 was used to discriminate the quality of the fit. All calculations were performed with WinSTAT® for Excel (R. Finch Software, 2015). Statistical significance was accepted if $p < 0.05$.

Results

Pachymetry

Average central corneal thickness in different swelling states are listed in Table 1. After reaching the steady state, higher hydrated corneas were significantly thicker compared to less hydrated corneas. The differences between all groups were statistical significant ($p < 0.05$) except between the 15 and 20% dextran group.

Surface-parallel extensiometry

The stress-strain curves show the typical nonlinear behavior of a corneal tissue, illustrated in Fig. 1. Corneas treated with 5% dextran showed the weakest behavior. With higher dextran concentrations (less hydrated) samples became stiffer with peak stresses in the 20% dextran group. At 6% strain, the 20% dextran-treated corneas were 3.8 times stiffer than 5% dextran-treated corneas ($p = 0.009$), resp. 2.6-fold stiffer than 10% dextran-treated corneas ($p = 0.009$), and 1.5-fold stiffer than 15% dextran-treated corneas ($p = 0.075$).

In order to calculate the tangential elastic modulus E^*, regression analysis was used to determine best-fit functions. Polynomials of third order achieved a higher coefficient of determination with $R^2 = 0.9999$ for all four examined hydration groups compared to other fitting approaches such as polynomials of second order (R^2 ranging from 0.9895 to 0.9933) or exponential (R^2 ranging from 0.9292 to 0.9552). The first derivative of the obtained third order polynomial at 6% strain allows to calculate a tangential elastic modulus E^* listed in Table 2.

Longitudinal Brillouin frequency shift

Brillouin frequency shifts averaged over the cornea are listed in Table 3. The differences are statistically different between all groups ($p = 0.004$). There was no measurable variation of

Table 1 Average minimal pachymetry with standard errors and calculated hydration (according to Eq. 1) after the establishment of an equilibrium

	5% dextran group	10% dextran group	15% dextran group	20% dextran group
Minimal central pachymetry [μm] ± SE	600 ± 31	473 ± 28	330 ± 10	305 ± 13
Hydration of the cornea [g water/g dry tissue] ± SE	4.57 ± 0.26	3.47 ± 0.24	2.23 ± 0.09	2.02 ± 0.11

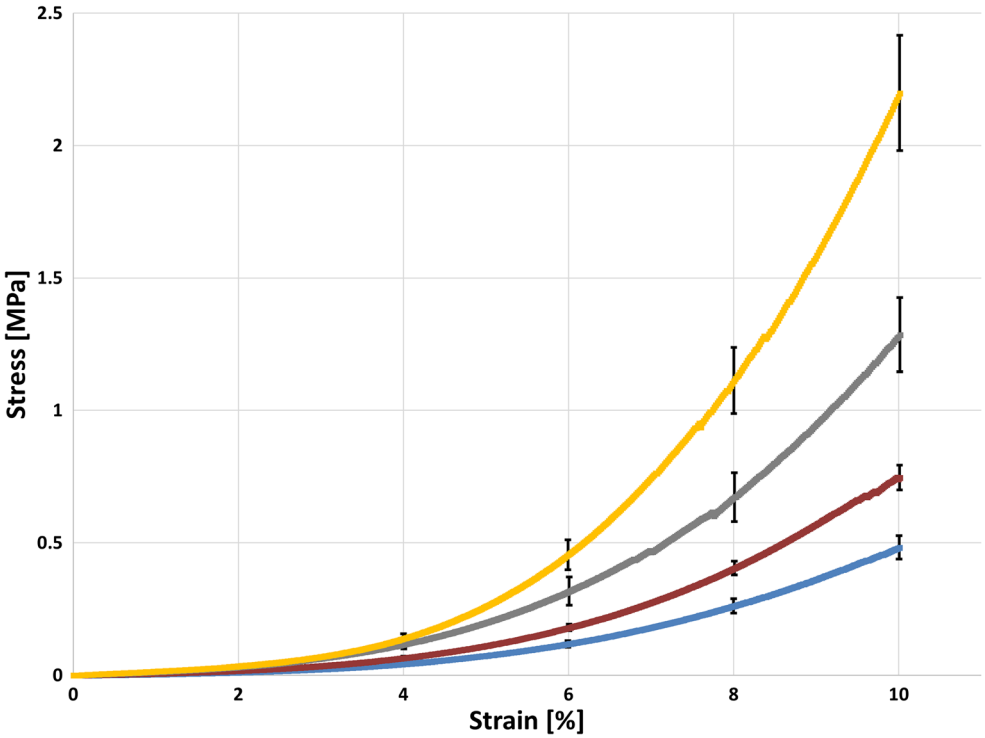

Fig. 1 Stress-strain relation for all hydration groups depicted up to 10% strain (yellow = 20% dextran, gray = 15% dextran, red = 10% dextran, blue = 5% dextran). Standard errors are added for even strains. Less hydrated corneas need higher stresses to achieve similar strains

Brillouin frequency shift within the corneal stroma, which is illustrated in Fig. 2 with representative axial scans of the four different groups. A decline is observed in the transition zone between posterior stoma and dextran solution in the anterior chamber. The moduli were calculated using Eq. 3 of Appendix A. Longitudinal Brillouin frequency shifts are negatively correlated with pachymetry (and therefore also negatively with hydration) with a correlation coefficient of $r = -0.965$ ($p = 0.017$).

The differences in Brillouin frequency shift, when varying the intraocular pressure in a 13% dextran group from 0 to 200 cm of water column (corresponding to the stress needed for an extension of 6% according to Laplace's law) were within the measurement error of ± 0.01 GHz. The values ranged from 5.560 to 5.568 GHz.

A plot of M versus E^* for all hydration groups allowed a comparison of the influence of hydration on the two different moduli E^* and M (Fig. 3). The linear fit achieved $R^2 = 0.946$ whereas the polynomial second-order fit achieved $R^2 = 0.999$.

Discussion

The major findings of this study are:

1. The longitudinal bulk modulus M of the rabbit cornea is at least 2 orders of magnitude higher than the tangential elastic modulus E*.
2. Increased corneal hydration decreases the tangential elastic modulus E* and the longitudinal bulk modulus M.
3. The elastic modulus E* is more sensitive in relative change on hydration changes than the bulk modulus M.
4. In contrast to the elastic modulus E*, the bulk modulus M seems to be independent on surface tension.

The here presented measurements of the bulk modulus of the cornea (Table 3) confirm the data of Scarcelli et al., who found a value of $M = 2.7 \pm 0.03$ GPa in bovine corneas of undocumented hydration [17]. Also, the values found for the surface-parallel elastic modulus E* ranging from 5 to 23 MPa

Table 2 Calculated hydrations according to Eq. 1 after the establishment of an equilibrium and the tangential elastic moduli E^* calculated at 6% strain for all four groups

	5% dextran group	10% dextran group	15% dextran group	20% dextran group
Hydration of the cornea [g water/g dry tissue] ± SE	4.57 ± 0.26	3.47 ± 0.24	2.23 ± 0.09	2.02 ± 0.11
E^* at 6% strain [MPa]	5.27	8.14	13.56	23.08

Table 3 Average Brillouin frequency shift and bulk modulus *M* of each group with standard error. Significantly higher Brillouin frequency shifts occur in less hydrated corneas

	5% dextran group	10% dextran group	15% dextran group	20% dextran group
Brillouin frequency shift [GHz] ± SE	5.33 ± 0.01	5.49 ± 0.01	5.63 ± 0.01	5.79 ± 0.03
Bulk modulus M [GPa] ± SE	2.45 ± 0.01	2.60 ± 0.01	2.74 ± 0.01	2.89 ± 0.03

fit nicely in the range of elastic moduli of 0.57–41 MPa published by Ziebarth [5]. The smaller values of $E < 1$ MPa were obtained mainly by acoustic force microscopy [16] or atomic force microscopy [19, 20], both measuring surface-perpendicular (longitudinal) moduli. Higher values of $M >$ 1 GPa origin from Brillouin frequency shift measurements [17, 18, 25, 26], a method that was introduced into experimental ophthalmology by Vaughn and Randall in 1980 [26]. However, Hatami-Marbini showed by means of unconfined compression experiments exactly the opposite: the surface-parallel elastic modulus of the porcine cornea is nearly three orders of magnitude bigger than the longitudinal (out-of-plane) modulus [33]. On the other hand, strip extensiometry has been shown to overestimate the material stiffness by approximately 30% compared to inflation testing [14]. The substantial numerical difference between longitudinal bulk modulus measured by Brillouin microscopy and tangential elastic moduli measured by extensiometry may be explained by the different mechanical mechanisms that constitute tensile and bulk moduli. As mentioned previously, also the time domain of the measurements differs: seconds in extensiometry compared to nanoseconds in Brillouin frequency shift detection [17]. Such a so-called dispersion of elastic moduli was measured also for the shear modulus of human cornea. Sörgel et al.

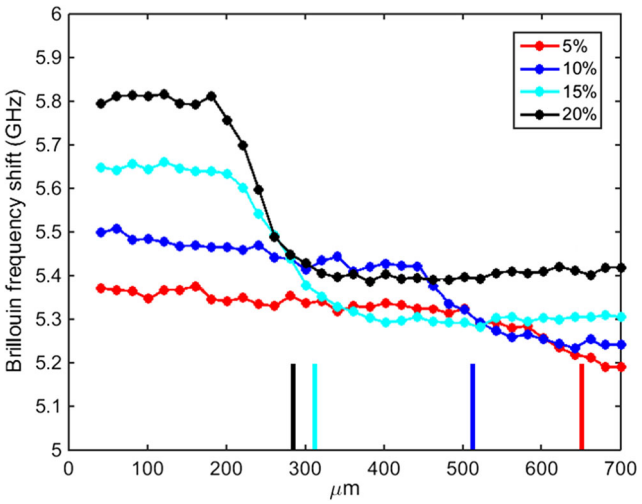

Fig. 2 Representative axial scans of Brillouin frequency shift within the corneal stroma of the four different hydration groups. The vertical bars represent the ultrasound pachymetry. Within the corneal stroma, the Brillouin frequency shift is constant showing a decay in the transition from posterior stroma to anterior chamber

measured a variation of two orders of magnitude in corneal shear modulus *G* when varying the shear frequency from 1 mHz to 100 Hz [27].

The relation of tangential and longitudinal (radial) strain during inflation testing was studied using ultrasound speckle tracking by Palko et al., who found a 2-fold higher radial compression compared to tangential strain [34]. To our best knowledge, we are the first group describing the quantitative relation between tangential elastic modulus E^* and longitudinal Brillouin bulk modulus *M* in cornea (Fig. 3). As biomechanical data acquisition so far is predominantly based on destructive ex vivo experiments, the here presented relation might become relevant for interpretation and comparison of experimental and in-vivo data. Previous attempts characterized such a relation of Brillouin bulk modulus with longitudinal compressive modulus [17, 18], but not with the tangential (surface-parallel) elastic modulus. As mentioned before, cornea is a highly anisotropic material [35, 36] that results in different biomechanical parameters in longitudinal and tangential directions.

Recently, Hatami-Marbini [11] investigated the influence of hydration on surface-parallel elastic modulus E^* in bovine corneas using uniaxial extensiometry. Although the setup differed in the preparation of the corneas, the results were very similar to ours with a factor of 6 between dehydrated and maximally hydrated corneas. This weakening is only partially explained by water storage within and in between the collagen fibers but also by the decrease in the number of stress-bearing elements per cross-section, as the cornea is thickened during the swelling process resulting in a lower stress value for the sample. This emphasizes the importance of controlled hydration conditions when performing cornea studies.

In corneal hydration levels higher than physiologic, additional water is mainly stored interfibrillar [37, 38]. Hence, the bulk modulus describing the longitudinal mechanical properties should be more sensitive to hydration compared to tangential elastic modulus. We were surprised that the here presented measurements indicate the opposite: E^* increases by factor of 4.4, whereas *M* increases only by a factor of 1.2 when decreasing corneal hydration.

The cornea is considered a nonlinear viscoelastic tissue [8], which implies that Hook's law is not valid, and an elastic modulus *E* must be defined in a different way. We chose the

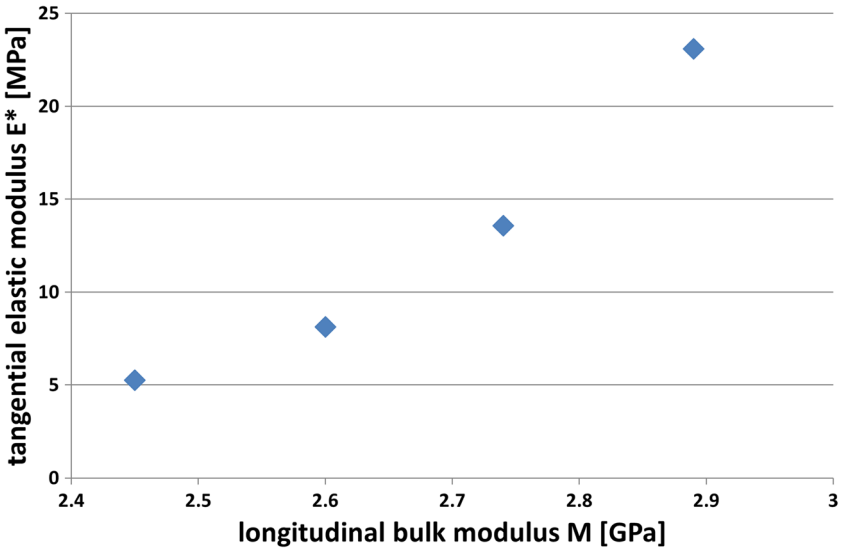

Fig. 3 Tangetial elastic modulus E^* versus longitudinal bulk modulus M in the four examined hydration groups at a strain of 6%. The polynomial second-order fit ($R^2 = 0.999$) seems to be superior to the linear fit ($R^2 = 0.946$)

tangential elastic modulus E^* defined as the first mathematical derivative of the stress-strain function. Since a polynomial of third order achieved the best fit, also this elastic modulus E^* is dependent on stress and strain. We chose for comparison reasons E^* at the strain of 6%. We and others [39–41] showed that tangential elastic moduli increase with stress and IOP, respectively. We could show for the first time, that the bulk modulus M determined by Brillouin spectroscopy is within the measurement error independent on stress and strain up to a strain of 6%. A possible explanation for this observation is that surface-parallel stress and strain is dominated by the macromolecular structure of the extracellular matrix of the cornea, whereas the bulk modulus describes the volume elasticity of the viscous part of the stroma [31] whose major component water is considered incompressible.

A weakness of the study is the assumption of an elastic system and the dispersion of the elastic moduli. Techniques using similar response frequencies for M and E^* would give more conclusive results but are unfortunately not available. Another limitation arises from the spatial averaging of the moduli throughout corneal thickness although the cornea is known to be vertically transverse isotropic: the anterior stroma appears to be stiffer compared to the posterior cornea [42]. On the other hand, we did not find a systematic difference between Brillouin shifts within the cornea. Lateral corneal anisotropy [24, 43] does not affect this study as extensiometry as well as Brillouin microscopy where only performed in the central cornea.

In conclusion, this publication investigates quantitatively the relation between the tangential elastic modulus E^* and the longitudinal bulk modulus M. In contrast to E^*, M is widely independent of stress and only minimally dependent of hydration of the cornea.

Acknowledgements The authors thank Irene E. Kochevar, PhD; Marleen Engler, BSc; and Eric Beck, BSc for their support.

Funding T. G. Seiler was supported by an unrestricted grant from the Swiss National Science Foundation. The sponsor had no role in the design or conduct of this research.

Compliance with ethical standards

Conflict of interest S.H. Yun is a co-founder of Intelon Inc., Boston, MA. T. Seiler and P. Shao are scientific consultants of Intelon Inc. T.G. Seiler and B.E. Frueh certify that they have no affiliations with or involvement in any organization or entity with any financial interest (such as honoraria; educational grants; participation in speakers' bureaus; membership, employment, consultancies, stock ownership, or other equity interest; and expert testimony or patent-licensing arrangements), or non-financial interest (such as personal or professional relationships, affiliations, knowledge, or beliefs) in the subject matter or materials discussed in this manuscript.

Ethical approval All applicable international, national, and institutional guidelines for the care and use of animals were followed.

Appendix A: Brillouin frequency shift and elastic module

Bulk Brillouin scattering can be used to probe elastic properties of transparent materials because incident light is inelastically scattered by acoustic wavelets (phonons) whose velocity is related with the elasticity of the material. Photons of the incident light may take energy from the phonons leading to wavelength shift (Stokes

shift) of the scattered light or may deliver energy to the phonons (anti-Stokes shift). Due to the experimental set-up, measuring backscattered light perpendicular to the corneal surface, only longitudinal waves can be measured and in this case the Brillouin frequency shift Ω can be expressed by

$$\Omega = \frac{2n}{\lambda} v \quad (1)$$

where n = refractive index of the medium, λ = wavelength, v = velocity of the acoustic wave [31]. Longitudinal ultrasound velocity v in isotropic media, on the other hand, is related with the bulk modulus M

$$M = \rho v^2 \quad (2)$$

where ρ = density of the medium. This bulk modulus M may not be confused with Young's elastic modulus E that describes the elastic properties in the surface-parallel plane. Combining Eqs. 1 and 2, it is obvious that $M \propto \Omega^2$, in detail

$$M = \rho \frac{\lambda^2 \Omega^2}{4 n^2} \quad (3)$$

For a physiologically hydrated cornea (equivalent to 13% dextran) the frequency shift Ω was 5.564 GHz. A density of $\rho = 1061$ kg/m^3, a laser wavelength of $\lambda = 780$ nm, and a refractive index of the corneal stroma $n = 1.3672$ yields for M a value of 2.673 GPa.

References

1. Maurice DM (1984) The cornea and the sclera. In: Davson H (ed) The Eye, Vol 1b, 3rd edn. Academic Press, Orlando, pp 1–158
2. Palko JR, Liu J (2016) Definitions and concepts. In: Roberts CJ, Liu J (eds) Corneal Biomechanics. Kugler Publications, Amsterdam, pp 1–24
3. Hatami-Marbini H, Maulik R (2016) A biphasic transversely isotropic poroviscoelastic model for the unconfined compression of hydrated soft tissue. J Biomech Eng 138:4032059
4. Thomsen L (1986) Weak elastic anisotropy. Geophysics 51:1954–1966
5. Dias J, Ziebarth NM (2015) Impact of hydration media on ex vivo corneal elasticity measurements. Eye Contact Lens 41:281–286
6. Liu J, Roberts CJ (2005) Influence of corneal biomechanical properties on intraocular pressure measurement: quantitative analysis. J Cataract Refract Surg 31:146–155
7. Spoerl E, Huhle M, Seiler T (1998) Induction of cross-links in corneal tissue. Exp Eye Res 66:97–103
8. Hoeltzel DA, Altman P, Buzard K, Choe K (1992) Strip extensiometry for comparison of the mechanical response of bovine, rabbit, and human corneas. J Biomech Eng 114:202–215
9. Hammer A, Richoz O, Mosquera SA, Tabibian D, Hoogewoud F, Hafezi F (2014) Corneal biomechanical properties at different corneal cross-linking (CXL) irradiances. Invest Ophth Vis Sci 55:2881–2884
10. Seiler TG, Fischinger I, Senfft T, Schmidinger G, Seiler T (2014) Intrastromal application of riboflavin for corneal crosslinking. Invest Ophthalmol Vis Sci 55:4261–4265
11. Hatami-Marbini H, Rahimi A (2015) Evaluation of hydration effects on tensile properties of bovine corneas. J Cataract Refract Surg 41:644–651
12. Boyce BL, Jones RE, Nguyen TD, Grazier JM (2007) Stress-controlled viscoelastic tensile response of bovine cornea. J Biomech 40:2367–2376
13. Elsheikh A, Alhasso D, Rama P (2008) Biomechanical properties of human and porcine corneas. Exp Eye Res 86:783–790
14. Elsheikh A, Anderson K (2005) Comparative study of corneal strip extensometry and inflation tests. J R Soc Interface 2:177–185
15. Gloster J, Perkins ES, Pommier ML (1957) Extensibility of strips of sclera and cornea. Br J Ophthalmol 41:103–110
16. Mikula ER, Jester JV, Juhasz T (2016) Measurement of an elasticity map in the human cornea. Invest Ophthalmol Vis Sci 57:3282–3286
17. Scarcelli G, Pineda R, Yun SH (2012) Brillouin optical microscopy for corneal biomechanics. Invest Ophthalmol Vis Sci 53:185–190
18. Webb JN, Su JP, Scarcelli G (2017) Mechanical outcome of accelerated corneal crosslinking evaluated by Brillouin microscopy. J Cataract Refract Surg 43:1458–1463
19. Dias JM, Ziebarth NM (2013) Anterior and posterior corneal stroma elasticity assessed using nanoindentation. Exp Eye Res 115:41–46
20. Seifert J, Hammer CM, Rheinlaender J, Sel S, Scholz M, Paulsen F, Schäffer TE (2014) Distribution of Young's modulus in porcine corneas after riboflavin/UVA-induced collagen cross-linking as measured by atomic force microscopy. PLoS One 9:e88186
21. Jue B, Maurice DM (1986) The mechanical properties of the rabbit and human cornea. J Biomech 19:847–853
22. Boyce BL, Grazier JM, Jones RE, Nguyen TD (2008) Full-field deformation of bovine cornea under constrained inflation conditions. Biomaterials 28:3896–3904
23. Kling S, Marcos S (2013) Effect of hydration state and storage media on corneal biomechanical response from in vitro inflation tests. J Refract Surg 29:490–497
24. Hjortdal JO (1996) Regional elastic performance of the human cornea. J Biomech 29:931–942
25. Scarcelli G, Kling S, Quijano E, Pineda R, Marcos S, Yun SH (2013) Brillouin microscopy of collagen crosslinking: noncontact depth-dependent analysis of corneal elastic modulus. Invest Ophthalmol Vis Sci 54:1418–1425
26. Vaughan JM, Randall JT (1980) Brillouin scattering, density and elastic properties of the lens and cornea of the eye. Nature 284:489–491
27. Soergel F, Jean B, Seiler T, Bende T, Mücke S, Pechhold W, Pels L (1995) Dynamic mechanical spectroscopy of the cornea for measurement of its viscoelastic properties in vitro. Ger J Ophthalmol 4:151–156
28. Petsche SJ, Chernyak D, Martiz J, Levenston ME, Pinsky PM (2012) Depth-dependent transverse shear properties of the human corneal stroma. Invest Ophthalmol Vis Sci 53:873–880
29. Spiru B, Kling S, Hafezi F, Sekundo W (2017) Biomechanical differences between femtosecond Lenticule extraction (FLEx) and small incision Lenticule extraction (SmILE) tested by 2D-Extensometry in ex vivo porcine eyes. Invest Ophthalmol Vis Sci 58:2591–2595
30. Scarcelli G, Yun SH (2016) Brillouin microscopy. In: Roberts CJ, Liu J (eds) Corneal Biomechanics. Kugler Publications, Amsterdam, pp 147–164

31. Reiß S, Burau G, Stachs O, Guthoff R, Stolz H (2011) Spatially resolved Brillouin spectroscopy to determine the rheological properties of the eye lens. Biomed Opt Express 2:2144–2159
32. Hedbys BO, Mishima S (1966) The thickness-hydration relationship of the cornea. Exp Eye Res 5:221–228
33. Hatami-Marbini H, Etebu E (2013) Hydration dependent biomechanical properties of the corneal stroma. Exp Eye Res 116:47–54
34. Palko JR, Tang J, Cruz Perez B, Pan X, Liu J (2014) Spatially heterogeneous corneal mechanical responses before and after riboflavin-ultraviolet-a crosslinking. J Cataract Refract Surg 40: 1021–1031
35. Müller LJ, Pels E, Schurmans LR, Vrensen GF (2004) A new three-dimensional model of the organization of proteoglycans and collagen fibrils in the human corneal stroma. Exp Eye Res 78:493–501
36. Nguyen TD, Jones RE, Boyce BL (2008) A nonlinear anisotropic viscoelastic model for the tensile behavior of the corneal stroma. J Biomech Eng 130:041020
37. Fratzl P, Daxer A (1993) Structural transformation of collagen fibrils in corneal stroma during drying. An x-ray scattering study. Biophys J 64:1210–1214
38. Meek KM, Fullwood NJ, Cooke PH, Elliott GF, Maurice DM, Quantock AJ, Wall RS, Worthington CR (1991) Synchrotron x-ray diffraction studies of the cornea, with implications for stromal hydration. Biophys J 60:467–474
39. Ko MW, Leung LK, Lam DC, Leung CK (2013) Characterization of corneal tangent modulus in vivo. Acta Ophthalmol 91:e263–e269
40. Singh M, Li J, Han Z, Wu C, Aglyamov SR, Twa MD, Larin KV (2016) Investigating elastic anisotropy of the porcine cornea as a function of intraocular pressure with optical coherence Elastography. J Refract Surg 32:562–567
41. Sperlich K, Reiß S, Bohn S, Stolz H, Guthoff RF, Jünemann A, Stachs O (2017) Effect of the age-related corneal elasticity on applanation tonometry. Klin Monatsbl Augenheilkd 234:1472–1476
42. Kohlhaas M, Spoerl E, Schilde T, Unger G, Wittig C, Pillunat LE (2006) Biomechanical evidence of the distribution of cross-links in corneas treated with riboflavin and ultraviolet a light. J Cataract Refract Surg 32:279–283
43. Elsheikh A, Brown M, Alhasso D, Rama P, Campanelli M, Garway-Heath D (2008) Experimental assessment of corneal anisotropy. J Refract Surg 24:178–187